Materials Science-Poland, 34(3), 2016, pp. 650-654
http://www.materialsscience.pwr.wroc.pl/
DOI: 10.1515/msp-2016-0075

DE GRUYTER OPEN

Synthesis of PVDF/SBT composite thin films by spin coating technology and their ferroelectric properties

CHANGCHUN CHEN*, PENGFEI HU, JUN YANG, ZIXUAN LIU

College of Materials Science and Engineering, Nanjing Tech University, NO.5 Xinmofan Road, Nanjing 210009, China

Ferroelectric composite thin films of x-SBT/PVDF with different SBT content (weight ratios of SBT to PVDF, x = 0 %, 5 %, 10 %, 15 %, 20 %) were prepared by spin-coating method. The crystal structures of x-SBT/PVDF films were analyzed by X-ray diffraction (XRD) measurements and Fourier transform-infrared spectroscopy (FT-IR), respectively. Experimental results demonstrated that both α, β-phases PVDF and the layered perovskite SBT co-existed in the x-SBT/PVDF samples. With an increase of SBT content in the x-SBT/PVDF thin films, both the dielectric constant and the saturated polarization were also increased, compared with those of pure PVDF thin film. More importantly, when the SBT content in the x-SBT/PVDF thin films was larger than 15 %, the coercive field of x-SBT/PVDF thin films was also decreased.

Keywords: *PVDF; SBT; ferroelectric composite films; remnant polarization*

1. Introduction

In recent years, great attention has been paid to poly(vinylidene fluoride) (PVDF) ferroelectric materials utilized by many devices, such as high energy density capacitors, pyroelectric thermal imaging devices, gate insulators in transistors, electro-optic light valves, thin-film memory elements, multiferroic transducers, energy harvesters, due to their useful dielectric, ferroelectric, piezoelectric properties together with their excellent stability to chemicals, mechanical flexibility and biocompatibility [1]. However, the shortcomings of PVDF ferroelectric polymer related to poorer ferroelectric properties and dielectric constant compared to those of ferroelectric ceramics have impeded the large scale utilization of pure PVDF polymer in the abovementioned ferroelectric devices. On the other hand, the ferroelectric ceramics, such as lead zirconate-titanate (PZT) with a conventional perovskite structure together with its compounds possessing high dielectric constant and high dipole moment, are the most widely used in commercial applications. In view of the toxicity of lead and its compounds, environmental friendly lead-free ferroelectric materials should be substantially employed in the field of ferroelectric devices [2]. Fortunately, strontium bismuth tantalate (SBT) with the layered perovskite structure is also widely used in the industry today. From the viewpoint of reliability, the SBT material offers superior characteristics over PZT material. The reason is that there exists polarization degradation in PZT ferroelectric devices [3]. In addition, compared to that of PZT, other advantages of SBT ferroelectric materials are better imprint characteristics, low voltage/low power operation and scaling potential. It is further worth noting that although both PZT and SBT materials are currently used for ferroelectric devices in commercial, industrial and radiation-hard applications, brittle structure and high temperature processing are the obstacles to their applications.

In order to fabricate a ferroelectric device with low cost, good chemical stability, superior mechanical and ferroelectric properties, a hybrid ceramic-polymeric composite should be a convenient solution to tune both mechanical and ferroelectric properties. The ferroelectric ceramic/PVDF composite materials would probably overcome

*E-mail: ccc@njtech.edu.cn

the defects of both polymeric materials and ferroelectric ceramics. So far, ferroelectric ceramic/PVDF composite materials, such as $BaTiO_3$(BT)/PVDF, $Pb(Zr,Ti)O_3$(PZT)/PVDF, have been investigated in the literature [4, 5]. In this study, SBT/poly (vinylidene fluoride) (SBT/PVDF) thin films were firstly prepared, and then the dependence of SBT content on the characteristics of x-SBT/PVDF (weight ratios of SBT to PVDF x = 0 %, 5 %, 10 %, 15 %, 20 %) thin films including structural, dielectric, ferroelectric properties was thoroughly investigated.

2. Experimental

2.1. Materials

Both PVDF powders and DMSO (dimethyl sulfoxide) solvents were supplied from Shanghai Ling Feng Chemical Reagent Co., Ltd. (China). The DMSO solvent was of reagent grade. $SrBi_2Ta_2O_9$(SBT) nanopowders were self-made. The detailed fabrication process of self-made SBT nanoparticles was described by Panda et al. [6].

2.2. Preparation of precursor solutions and thin films

The x-SBT/PVDF(x = 0 %, 5 %, 10 %, 15 %, 20 %) thin films were prepared by a spin-coating method. The x was the weight ratio of SBT corresponding to PVDF in the thin film. The different amounts of PVDF were separately dissolved in DMSO solvent at a fixed volume in different flasks. In order to get the fully dissolved PVDF solutions, the solutions in different flasks were magnetically stirred at 60 °C in a water-bath heater. Meanwhile, the self-made SBT nanoparticles in different weights were also added into the DMSO solvent in the flasks, followed by ultrasonic stirring for 20 minutes to obtain homogeneous SBT suspensions for the next step spinning process. Finally, the PVDF solutions were poured into the SBT suspensions with different weight ratios of SBT to PVDF and subsequently vigorously mixed with a rotating stirrer accompanying by ultrasounds for 20 minutes with an aim to obtaining homogeneous suspensions.

During the fabrication of x-SBT/PVDF (x = 0 %, 5 %, 10 %, 15 %, 20 %) thin films, the PVDF/SBT suspension precursors were firstly spin-coated on the cleaned ITO coated glass substrate (having resistance 60 Ω/sq to 120 Ω/sq) and crystalline Si substrate at a rate of 4000 rpm for 30 s, respectively. It should be pointed out in this study that the x-SBT/PVDF film samples grown on Si substrate were used to determine the crystal structure of the films via XRD analysis whereas the x-SBT/PVDF films grown on the ITO coated glass substrate were used to characterize the electrical properties of the films. Then the formed wet films were transferred into an air blowing thermostatic oven with temperature of 60 °C for evaporating the solvent. The coating and thermal treatment process were repeated ten times in order to obtain the films of a certain thickness. The resultant films were then placed into the air blowing thermostatic oven under 60 °C for 48 hours. When they were naturally cooled down to room temperature, these x-SBT/PVDF thin films were successfully fabricated.

2.3. Structural and electrical characterizations

The crystal structure properties of x-SBT/PVDF films on Si substrate synthesized in this study were investigated by θ to 2θ method of XRD with a $CuK\alpha_1$ ($\lambda = 0.15406$ nm) source at 40 kV and 35 mA using an ARL XTRA powder X-ray diffraction diffractometer at a scan rate of 10°/min. FT-IR spectra were performed on a Nicolet FT-IR spectrophotometer (Nexus 470, Thermo Electrcon Corporation) using KBr disks at room temperature. For electrical measurements, silver with about 300 nm thickness was coated on the surface of the x-SBT/PVDF membranes on the ITO coated glass substrate with an area of 5.25×10^{-5} cm^{-2} using a shadow mask. The ferroelectric hysteresis loops and leakage currents of the Ag/x-SBT/PVDF/ITO capacitors were obtained using a ferroelectric tester (Radiant Technologies, Precision LC). The dielectric constant and the dissipation factors were measured by using an HP4294A impedance analyzer. The high-frequency capacitance-voltage

characteristics of these samples were measured using Keithley 590 CV analyzer at one MHz with a bias sweep rate of 0.2 V/s. All the measurements were performed at room temperature.

3. Results and discussion

3.1. XRD and FT-IR analyses

Fig. 1 shows the XRD patterns of the x-SBT/PVDF (x = 0 %, 5 %, 10 %, 15 %, 20 %) films on Si substrate. The peaks corresponding to SBT and PVDF have been denoted by various symbols. The peaks at 2θ = 28.91° and 32.40° associated with the reflection planes of (1 1 5), (2 0 0) are assigned to the layered perovskite phase respectively of the SBT shown in Fig. 1a. Meanwhile, the peaks at 2θ = 19.7° and 21.6°, ascribed to α and β phases of PVDF, are denoted in Fig. 1b, respectively [7]. The crystallite size of SBT nanoparticles was found to be nearly 31 nm which was calculated by Scherrer's formula: $d = \frac{k\lambda}{\beta \cos\theta}$, where k is the shape factor (k = 0.94), λ is the X-ray wavelength, β is the line broadening at half maximum intensity (FWHM) in radius, θ is the Bragg's angle, and d is the crystallite size. In the pure PVDF film (x = 0) sample fabricated in this study, only α phase of PVDF is found. With an increase of x in the x-SBT/PVDF films in the range from x = 0 % to 20 % at a 5 % interval, the β phase of PVDF appeared and it is demonstrated in Fig. 1 [8]. In other words, the addition of SBT into the PVDF was favorable to the formation of the β phase of PVDF owing to the more regular alignment of PVDF chain under the thermal processing conditions in this study. The structural characteristics of x-SBT/PVDF (x = 0 %, 5 %, 10 %, 15 %, 20 %) films on ITO coated glass substrate were further investigated by FI-IR spectra shown in Fig. 2. The characteristic absorption bands of α-phase PVDF are at 531, 764 and 989 cm^{-1}, while β-phase has characteristic absorption bands at 840 cm^{-1} and 1274 cm^{-1}, which are marked in Fig. 2 [9, 10]. Absorption lines appreciably appeared at around 505, 617, and 802 cm^{-1} which corresponds to Bi–O, Sr–O, and Ta–O vibrational absorption mode [11, 12]. The results obtained from XRD and FT-IR indicate that α- and β-phase of PVDF, and the layered perovskite SBT co-exist in the x-SBT/PVDF samples.

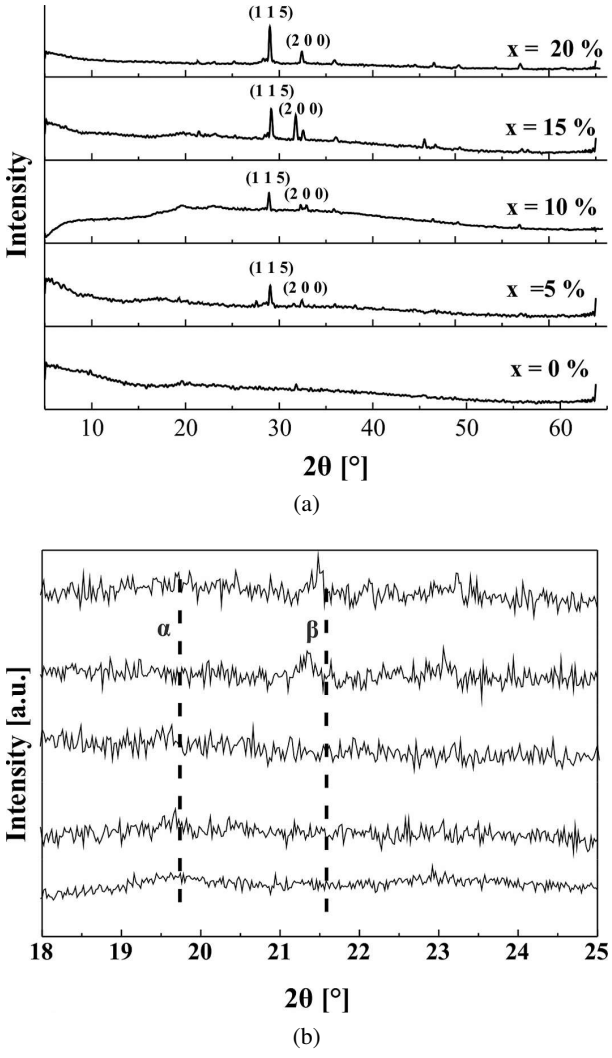

Fig. 1. XRD patterns of the x-SBT/PVDF films (x =0 %, 5 %, 10%, 15 %, 20 %) on Si substrate: (a) full spectra; (b) partial spectra with amplification image (diffraction angle from 18° to 25°).

3.2. Dependence of dielectric constant on frequency

The variations of dielectric constant as a function of frequency in the range from 5 kHz to 100 kHz for the x-SBT/PVDF films on ITO coated glass substrate measured at room temperature are shown in Fig. 3. It can be observed that with an increase of SBT content in the x-SBT/PVDF thin films, the dielectric constants of x-SBT/PVDF also

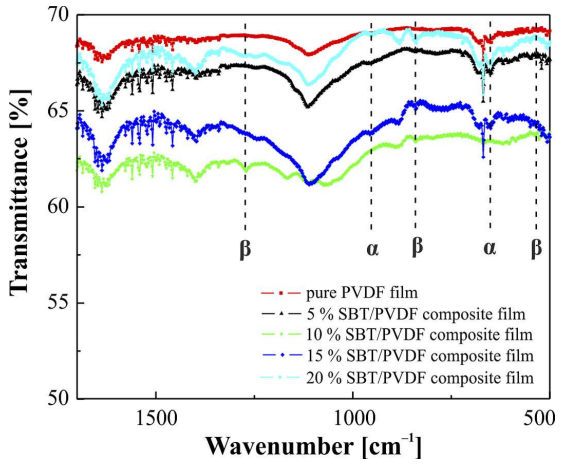

Fig. 2. FT-IR spectra of the x-SBT/PVDF films (x = 0 %, 5 %, 10 %, 15 %, 20 %) on ITO coated glass substrate.

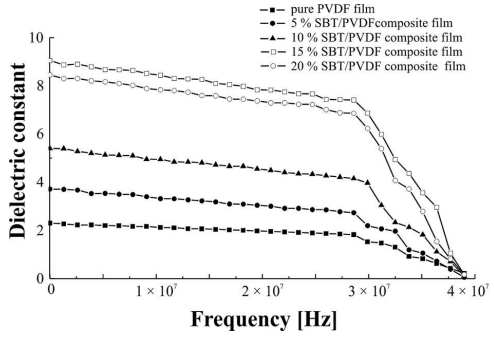

Fig. 3. Frequency dependence of the relative dielectric constant of the x-SBT/PVDF(x = 0 %, 5 %, 10 %, 15 %, 20 %) films on ITO coated glass substrate measured at room temperature.

increase. What's more, for all the x-SBT/PVDF films, the value of dielectric constant was high at lower frequencies and decreased with an increase in frequency. The characteristics can be explained according to the space-charge relaxation phenomena wherein at low frequencies the space charges are able to follow the frequency of applied field while at a higher frequency, they may not have time to undergo relaxation [13].

3.3. Ferroelectric properties

The polarization-electric field (P-E) hysteresis loops of the x-SBT/PVDF films on ITO coated glass substrate, measured under the applied electric field up to 110 kV/cm are shown in Fig. 4. For the pure PVDF film, a ferroelectric hysteresis loop is observed with saturated polarization of 1.98 μC/cm^2 measured under the electric field of 110 kV/cm. With an increase of SBT content (x) in the x-SBT/PVDF composite thin films, the saturated polarization of the x-SBT/PVDF films is also gradually enhanced. Compared to its counterpart, the x-SBT/PVDF (x = 20 %) film has the largest saturated polarization of 9.02 μC/cm^2. Owing to the saturated polarization of SBT being larger than that of PVDF, the enhanced saturated polarization existing in the x-SBT/PVDF thin films is probably ascribed to the addition of SBT into the x-SBT/PVDF films. As the saturated polarization of x-SBT/PVDF thin films is higher than that of pure PVDF, it can be concluded that the power generating capability of x-SBT/PVDF will also be higher than that of pure PVDF. On the other hand, with an increase of SBT content (x) in the x-SBT/PVDF composite films, the PVDF chains become more regularly aligned, which is demonstrated by XRD spectra together with FT-IR spectra shown in Fig. 1 and Fig. 2, respectively. Consequently, the coercive field of x-SBT/PVDF thin films gradually increases from 23.8 kV/cm (x = 0 %) to 48.6 kV/cm (x = 0.15 %), and finally decreases to 37.4 kV/cm (x = 0.20).

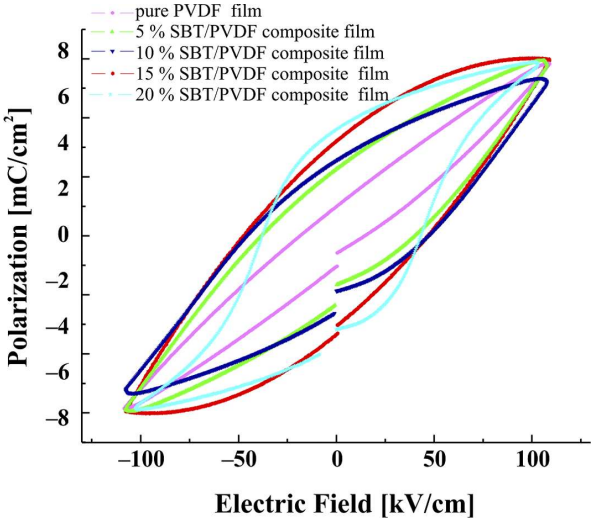

Fig. 4. Electric hysteresis loops of the x-SBT/PVDF (x = 0 %, 5 %, 10 %, 15 %, 20 %) films on ITO coated glass substrate.

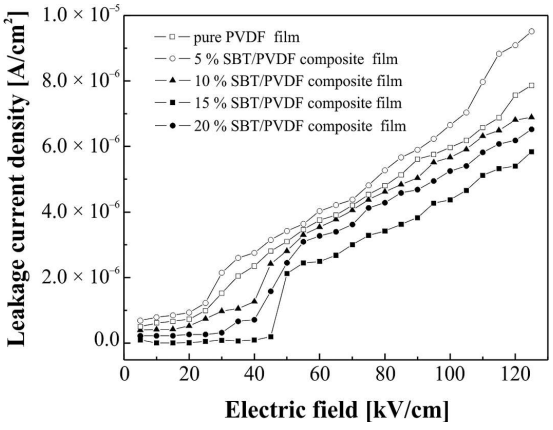

Fig. 5. I-V characteristics of the x-SBT/PVDF (x = 0 %, 5 %, 10 %, 15 %, 20 %) films on ITO coated glass substrate.

3.4. Current density

The variation in the current density with applied electrical filed for x-SBT/PVDF(x = 0 %, 5 %, 10 %, 15 %, 20 %) films on ITO coated glass substrate measured at room temperature is shown in Fig. 5. The magnitude of current density was 9.7×10^{-6} A/cm^2 for pure PVDF film (x = 0 %) at 125 kV/cm. With the increase of SBT content in the x-SBT/PVDF films, the current density in the films under the applied electrical field firstly decreased and then increased. This behavior could be explained as follows. When the amount of SBT added to the PVDF matrix was low, the regular PVDF chains alignment could improve the crystalline structure of the x-SBT/PVDF films. As a result, the leakage current densities in the films were also reduced. However, when the amount of SBT content in the x-SBT/PVDF thin film was larger than or equal to 0.2, the addition of SBT into the PVDF matrix could destroy the regularity of PVDF chain and bring about more defects into film (Fig. 3). Hence, compared to its counterpart, the leakage current density of x-SBT/PVDF (x = 15 %) film with magnitude of 5.8×10^{-6} A/cm^2 was the least.

4. Conclusions

In this paper, we reported the preparation of ferroelectric x-SBT/PVDF (x = 0 %, 5 %, 10 %, 15 %, 20 %) films by spin-coating method. The structural characteristic of the resulting films were determined by XRD, FT-IR. Both α- and β-phase of PVDF, and the layered perovskite SBT co-existed in the x-SBT/PVDF samples. With an increase of SBT content in x-SBT/PVDF films, the values of dielectric constant of the films also increased. The polarization-electric field loop exhibited enhanced saturated polarization from 1.98 μC/cm^2 to 9.02 μC/cm^2. Meantime, the SBT nanoparticles added into the PVDF matrix could degrade the leakage current of the x-SBT/PVDF films under the applied electric field. These results indicate that the x-SBT/PVDF composite film with adjustable ferroelectric properties could probably be favorable for future applications ranging from broadband sensing to flexible energy scavenging.

Acknowledgements

This study is financed by the Priority Academic Program Development of Jiangsu Higher Education Institutions (PAPD), China.

References

[1] FURUKAWA, NAKAJIMA T., TAKAHASHI Y., *IEEE T. Dielec. El. In.*, 13 (2006), 1120.
[2] KHACHATURYAN A.G., *Philos. Mag*, 90 (2010), 37.
[3] GOUX L., MAES D., LISONI J.G., MEEREN VAN DER H., PARASCHIV V., HASPESLAGH L., ARTONI C., RUSSO G., ZAMBRANO R., WOUTERS D.J., *Microelectron. Eng.*, 83 (2006), 2027.
[4] FANG F., YANG W., ZHANG M.Z., WANG Z., *Compos. Sci. Technol.*, 69 (2009), 602.
[5] ZAK A.K., GAN W.C., MAJID W.H.A., DARROUDI M., VELAYUTHAM T.S., *Ceram. Int.*, 37 (2011), 1653.
[6] PANDA A.B., TARAFDAR A., PRAMANIK P., *J. Eur. Ceram. Soc.*, 24 (2004), 3043.
[7] MOHAJIR B.E., HEYMANS N., *Polymer*, 42 (2001), 5661.
[8] YE C., DECAI Y., *Acta Polym. Sin.*, 10 (1995), 519.
[9] BORMASHENKO Y., POGREB R., STANEVSKY O., BORMASHENKO E., *Polym. Test.*, 23 (2004), 791.
[10] KOBAYASHI M., TASHIRO K., TADOKORO H., *Macromolecules*, 8 (1975), 158.
[11] KE H., ZHOU Y., JIA D.C., WANG W., XU X.Q., *J. Sol-Gel Sci. Techn.*, 34 (2005), 131.
[12] NISHIZAWA K., MIKI T., SUZUKI K., KATO K., *J. Mater. Res.*, 18 (2003), 899.
[13] SAHU J.R., RAO C.N.R., *Solid State Sci.*, 9 (2007), 950.

Received 2016-01-20
Accepted 2016-06-01